Reduced order modeling and analysis of the human complement system

Adithya Sagar, Wei Dai[#], Mason Minot[#], and Jeffrey D. Varner[*]

School of Chemical and Biomolecular Engineering

Cornell University, Ithaca NY 14853

Running Title: A reduced order model of complement

To be submitted: *Scientific Reports*

[#] Denotes equal contribution

[*]Corresponding author:

Jeffrey D. Varner,

Professor, School of Chemical and Biomolecular Engineering,

244 Olin Hall, Cornell University, Ithaca NY, 14853

Email: jdv27@cornell.edu

Phone: (607) 255 - 4258

Fax: (607) 255 - 9166

Abstract

Complement is an important pathway in innate immunity, inflammation, and many disease processes. However, despite its importance, there have been few validated mathematical models of complement activation. In this study, we developed an ensemble of experimentally validated reduced order complement models. We combined ordinary differential equations with logical rules to produce a compact yet predictive complement model. The model, which described the lectin and alternative pathways, was an order of magnitude smaller than comparable models in the literature. We estimated an ensemble of model parameters from *in vitro* dynamic measurements of the C3a and C5a complement proteins. Subsequently, we validated the model on unseen C3a and C5a measurements not used for model training. Despite its small size, the model was surprisingly predictive. Global sensitivity and robustness analysis suggested complement was robust to any single therapeutic intervention. Only dual dual-knockdown of both C3 and C5 consistently reduced C5a formation when all pathways were activated. Taken together, we developed a reduced order complement model that was computationally inexpensive, and could easily be incorporated into pre-existing or new pharmacokinetic models of immune system function. The model described experimental data, and predicted the need for multiple points of therapeutic intervention to disrupt complement activation.

Keywords: Complement system, systems biology, reduced order models, biochemical engineering

Introduction

Complement is an important pathway in innate immunity. It plays a significant role in inflammation, host defense as well as many disease processes. Complement was discovered in the late 1880s where it was found to 'complement' the bactericidal activity of natural antibodies (1). However, research over the past decade has shown that the importance of complement extends well beyond innate immunity. For example, complement contributes to tissue homeostasis by inducing tissue repair (2). Complement has also been linked with several diseases including Alzheimers, Parkinson's disease, multiple sclerosis, schizophrenia, rheumatoid arthritis and sepsis (3, 4). Complement plays both positive and negative roles in cancer; attacking tumor cells with altered surface proteins in some cases, while potentially contributing to tumor growth in others (5, 6). Lastly, several other important biochemical subsystems are integrated with complement including the coagulation cascade, the autonomous nervous system and inflammation (6). Thus, complement is important in a variety of beneficial and potentially harmful functions in the body.

The complement cascade involves over 30 soluble and cell surface proteins, receptors and regulators. The molecular connectivity of complement involves both fluid phase and cell surface events, see the review of Walport (7, 8). The central outputs of complement are the Membrane Attack Complex (MAC), and the inflammatory mediator proteins C3a and C5a. The membrane attack complex, generated during the terminal phase of the response, forms transmembrane channels which disrupt the membrane integrity of targeted cells, leading to cell lysis and death. On the other hand, the C3a and C5a proteins act as a bridge between innate and adaptive immunity, and play an important role in regulating inflammation (5). Complement activation takes places through three pathways: the classical, the lectin binding and the alternate pathways. The classical pathway is triggered by antibody recognition of foreign antigens or other pathogens. A multimeric protein com-

plex C1 binds to antibody-antigen complexes and undergoes a conformational change, leading to an activated form with proteolytic activity. This activated complex then cleaves soluble complement proteins C4 and C2 into C4a, C4b, C2a and C2b, respectively. The C4a and C2b fragments bind to form the C4bC2a protease, also known as the classical C3 convertase. The lectin pathway is initiated through the binding of L-ficolin or Mannose Binding Lectin (MBL) to carbohydrates on the surfaces of bacterial pathogens. These complexes, in combination with the associated mannose-associated serine proteases 1 and 2 (MASP-1/2), also cleave C4 and C2, leading to additional classical C3 convertase. Thus, the classical and lectin pathways, initiated by the recognition of different cues on foreign surfaces, converge at the classical C3 convertase. However, the alternate pathway works differently. It is activated by a 'tickover' mechanism in which complement protein C3 is spontaneously hydrolyzed to form an activated intermediate C3w; C3w recruits factor B and factor D, leading to the formation of C3wBb. C3wBb cleaves C3 into C3a and C3b, where the C3b fragment further recruits additional factor B and factor D to form C3bBbC3b, the alternate C3 convertase (9). The role of classical and alternate C3 convertases is varied. First, C3 convertases mediate signal amplification. C3 convertases cleave C3 into C3a and C3b; the C3b fragment is then free to form additional alternate C3 convertases, thereby forming a positive feedback loop. Next, C3 convertases link complement initiation with the terminal phase of the cascade through the formation of C5 convertases. Both classical and alternate C3 convertases can recruit C3b subunits to form the classical C5 convertase (C4bC2aC3b), and the alternate C5 convertase (C3bBbC3b), respectively. C5 convertases cleave C5 into the C5a and C5b fragments. The C5b fragment, along with the C6, C7, C8 and multiple C9 complement proteins, form the membrane attack complex. On the other hand, both C3a and C5a are important inflammatory signals involved in several responses (7, 8). Thus, the complement cascade directly attacks the invading pathogen, and signals for help from the immune system.

The complement cascade is regulated by plasma and host cell proteins which balance host cell safety with effectiveness. The initiation of the classical pathway via complement protein C1 is controlled by the C1 Inhibitor (C1-Inh). C1-Inh irreversibly binds to and deactivates the active subunits of C1, preventing chronic complement activation (10). Regulation of upstream processes in the lectin and alternate pathways also occurs through the interaction of the C4 binding protein (C4BP) with C4b, and factor H with C3b (11). Interestingly, both factor H and C4BP are capable of binding their respective targets while in convertase complexes as well. At the host cell surface, membrane cofactor protein (MCP or CD46) can interact with C4b and C3b, which protects the host cell from complement self-activation (12). Delay accelerating factor (DAF or CD55) also recognizes and dissociates both C3 and C5 convertases on host cell surfaces (13). More generally, Carboxypeptidase-N, a well known inflammation regulator, has broad activity against the complement proteins C3a, C4a, and C5a, rendering them inactive by cleavage of carboxyl-terminal arginine and lysine residues (14). Although Carboxypeptidase-N does not directly influence complement activation, it silences the important inflammatory signals produced by complement. Lastly, the assembly of the MAC complex itself can be inhibited by vitronectin and clusterin in the plasma, and CD59 at the host surface (15, 16). Thus, there are many points of control which influence complement across the three activation pathways.

Developing quantitative mathematical models of complement will be crucial to fully understanding its role in the body. Traditionally, complement models have been formulated as systems of linear or non-linear ordinary differential equations (ODEs). For example, Hirayama et al. modeled the classical complement pathway as a system of linear ODEs (17), while Korotaevskiy and co-workers modeled the classical, lectin and alternate pathways (up to C3a) as a system of non-linear ODEs (18). More recently, large mechanistic models of sections of complement have also been proposed. For example, Liu et al. an-

3

alyzed the formation of the classical and lectin C3 convertases, and the regulatory role of C4BP using a system of 45 non-linear ODEs with 85 parameters (19). Zewde and co-workers constructed a detailed mechanistic model of the alternative pathway which consisted of 107 ODEs and 74 kinetic parameters and delineated between the host cell and pathogen (16). However, these previous modeling studies involved little experimental validation. Thus, while these models are undoubtably important theoretical tools, it is unclear if they can describe or quantitatively predict complement measurements. The central challenge of complement model identification is the estimation of model parameters from experimental measurements. Unlike other important cascades, such as coagulation where there are well developed experimental tools and publicly available data sets, the data for complement is relatively sparse. Missing or incomplete data sets, and limited quantitative data make the identification of large mechanistic complement models difficult. Thus, reduced order modeling approaches, which describe the key biology with a limited number of parameters, will be important for developing validated models of complement, and to fully understandings its role in the body.

Results

In this study, we developed an ensemble of experimentally validated reduced order complement models. The modeling approach combined ordinary differential equations with logical rules to produce a complement model with a limited number of equations and parameters. The reduced order model, which described the lectin and alternative pathways, consisted of 18 differential equations with 28 parameters. Thus, the model was an order of magnitude smaller and included more pathways than comparable models in the literature. We estimated an ensemble of model parameters from *in vitro* time series measurements of the C3a and C5a complement proteins. Subsequently, we validated the model on unseen C3a and C5a measurements that were not used for model training. Despite its small size, the model was surprisingly predictive. After validation, we performed global sensitivity and robustness analysis to estimate which parameters and species controlled model performance. These analyses suggested complement was robust to any single therapeutic intervention; only the knockdown of both C3 and C5 consistently reduced C3a and C5a formation for all cases. Taken together, we developed a reduced order complement model that was computationally inexpensive, and could easily be incorporated into pre-existing or new pharmacokinetic models of immune system function. The model described experimental data, and predicted the need for multiple points of intervention to disrupt complement activation.

Reduced order complement network. The complement model described the alternate and lectin pathways (Fig. 1). A trigger event initiated the lectin pathway, which activated the cleavage of C2 and C4 into C2a, C2b, C4a and C4b respectively. Classical Pathway (CP) C3 convertase (C4aC2b) then catalyzed the cleavage of C3 into C3a and C3b. The alternate pathway was initiated through the spontaneous hydrolysis of C3 into C3a and C3b (not C3w). The C3b fragment generated by hydrolysis (or by CP C3 convertase) could then form the alternate pathway (AP) C3 convertase (C3bBb). We did not consider

5

C3w, nor the formation of the initial alternate C3 convertase (C3wBb). Rather, we assumed C3w was equivalent to C3b and only modeled the formation of the main AP C3 convertase. Both the CP and AP C3 convertases catalyzed the cleavage of C3 into C3a and C3b. A second C3b fragment could then bind with either the CP or AP C3 convertase to form the CP or AP C5 convertase (C4bC2aC3b or C3bBbC3b). Both C5 convertases catalyzed the cleavage of C5 into the C5a and C5b fragments. In this initial study, we simplified the model by assuming both Factor B and Factor D were in excess. However, we did explicitly account for two control proteins, Factor H and C4BP. Lastly, we did not consider MAC formation, instead we stopped at C5a and C5b. Lectin pathway activation, and C3/C5 convertase activity was modeled using a combination of saturation kinetics and non-linear transfer functions, which facilitated a significant reduction in the size of the model while maintaining performance. Binding interactions were modeled using mass-action kinetics, where we assumed all binding was irreversible. Thus, while the reduced order complement model encoded significant biology, it was highly compact consisting of only 18 differential equations and 28 model parameters. Next, we estimated an ensemble of model parameters from time series measurements of the C3a and C5a complement proteins.

Estimating an ensemble of reduced order complement models. A critical challenge for the development of any dynamic model is the estimation of model parameters. We estimated an ensemble of complement model parameters in a hierarchical fashion using *in vitro* time-series data sets generated with and without zymosan, a lectin pathway activator (20). The residual between model simulations and experimental measurements was minimized using the dynamic optimization with particle swarms (DOPS) routine, starting from an initial random parameter guess. Unless otherwise specified, all initial conditions were assumed to be their mean physiological values. A hierarchical approach was taken in which the alternate pathway parameters were estimated first and then fixed during the

6

estimation of the lectin pathway parameters. While we had significant training data, the parameter estimation problem was underdetermined (we were not able to uniquely determine model parameters). Thus, instead of using a best-fit yet uncertain parameter set, we estimated an ensemble of probable parameter sets (N = 50, see materials and methods). The reduced order complement model ensemble captured the behavior of both the alternative and lectin pathways (Fig. 2). For the alternative pathway, we used C3a and C5a measurements in the absence of zymosan, and only allowed the alternative parameters to vary (Fig. 2A and B). On the other hand, lectin pathway parameters were estimated from C3a and C5a measurements in the presence of 1g zymosan with alternate pathway parameters fixed (Fig. 2C and D). The reduced order model reproduced a panel of alternate and lectin pathway data sets in the neighborhood of physiological factor and inhibitor concentrations. However, it was unclear whether the reduced order model could predict new data, without updating the model parameters. To address this question, we fixed the model parameters and simulated data sets not used for model training.

We tested the predictive power of the reduced order complement model with data not used during model training (Fig. 3). Six validation cases were considered, three for C3a and C5a, respectively. All model parameters and initial conditions were fixed for the validation simulations (with the exception of zymosan, and other experimentally mandated changes). The ensemble of reduced order models predicted the qualitative dynamics of C3a formation (Fig. 3, top), and C5a formation (Fig. 3, bottom) at three inducer concentrations. The rate of C3a formation and C3a peak time were directly proportional to initiator dose. Similarly, the C5a plateau and rate of formation were also directly proportional to initiator dose, with the lag time being indirectly proportional to initiator exposure. However, there were shortcomings with model performance. First, while the overall C3a trend was captured (within the 99% confidence interval), the C3a dynamics were too fast with the exception of the low dose case. We believe the C3a timescale was related to

7

our choice of training data, how we modeled the tickover mechanism, and factor B and D limitation. We trained the model using either no or 1 mg/ml zymosan, but predicted cases in a different initiator range; comparing the training to prediction, the model performance e.g., the shape of the C3a trajectory was biased towards either high or very low initiator doses. Next, tickover was modeled as a first-order generation processes where C3wBb formation and activity was lumped into the AP C3 convertase. Thus, we skipped an important step which could strongly influence AP C3 convertase formation by slowing down the rate C3 cleavage into C3a and C3b. We also assumed both factor B and factor D were not limiting, thereby artificially accelerating the rate of AP C3 convertase formation. The C5a predictions followed a similar trend as C3a; we captured the long-time C5a behavior but over predicted the time scale of C5 cleavage. However, because the C5a time scale depends strongly upon C3 convertase formation, we can likely correct the C5 issues by fixing the rate of C3 cleavage. Despite these shortcomings, we qualitatively predicted unseen experimental measurements within the 99% confidence of the ensemble, for three inducer levels. Next, we used global sensitivity and robustness analysis to determine which parameters and species controlled the performance of the complement model.

Global analysis of the reduced order complement model. We conducted sensitivity analysis to estimate which parameters controlled the performance of the reduced order complement model. We calculated the total sensitivity of the C3a and C5a residual to changes in model parameters with and without zymosan (Fig. 4). In the absence of zymosan (where only the alternative pathway is active), the most sensitive parameter was the rate constant governing the assembly of the AP C3 convertase, as well as the rate constant controlling basal C3b formation. The C5a trajectory was sensitive to the AP C5 convertase kinetic parameters (Fig. 4A). Interestingly, neither the rate nor the saturation constants governing AP C3-convertase activity were sensitive in the absence of zymosan. Thus, C3a formation in the alternative pathway was more heavily influenced by

8

the spontaneous hydrolysis of C3, rather than AP C3-convertase activity, in the absence of zymosan. In the presence of zymosan, the C3a residual was controlled by the formation and activity of the CP C3 convertase, as well as tickover and degradation parameters. On the other hand, the C5a residual was controlled by the formation and activity of CP C5 convertase, and tickover C3b formation in the presence of zymosan (Fig. 4B). The lectin initiation parameters were sensitive, but to a lesser extent than CP convertase kinetic parameters and tickover C3b formation. Thus, sensitivity analysis suggested that CP C3/C5 convertase formation and activity dominated in the presence of zymosan, but tickover parameters and AP C5 convertase were more important without initiator. Next, we compared the sensitivity results to current therapeutic approaches; pathways involving sensitive parameters have been targeted for clinical intervention (Fig. 4C). In particular, the sensitivity analysis suggested AP/CP C5 convertase inhibitors, or interventions aimed at attenuating C3 or C5 would most strongly influence complement performance. Thus, there was at least a qualitative overlap between sensitivity and the potential of biochemical efficacy. However, sensitivity coefficients are only a local measure of how small changes in parameters affect model performance. To more closely simulate a clinical intervention e.g., administration of an anti-complement inhibitor, we performed robustness analysis.

Robustness coefficients quantify the response of a marker to a macroscopic structural or operational perturbation to a biochemical network. Here, we computed how the C3a and C5a trajectories responded to a decrease in the initial abundance of C3 and/or C5. Robustness analysis suggested there was no single intervention that inhibited complement activation in the presence of both initiation pathways (Fig. 5). We calculated robustness indices for C3a and C5a for the parameter ensemble (N = 50) with and without the lectin pathway initiator. We simulated the addition of different doses of anti-complement inhibitor cocktails by decreasing the initial concentration of C3 or C5 or the combination of C3 and C5 by 50% and 90%. This would be conceptually analogous to the administration

9

of a C3 inhibitor e.g., compstatin alone or combination with eculizumab (Fig. 4E). A $\log_{10}$ transformed robustness index of zero indicated no effect due to the perturbation, whereas an index of less than zero indicated decreased C3a or C5a. The response of the complement model to different knock-down magnitudes was non-linear; a 90% knock-down had an order of magnitude more impact than a 50% knock-down. As expected, a C5 knock-down had no effect on C3a formation for either the alternate (Fig. 5A, lanes 1 or 3) or lectin pathways (Fig. 5B, lanes 1 or 3). However, C3a abundance and to a lesser extent C5a abundance decreased with decreasing C3 concentration in the alternate pathway (Fig. 5A or B, lanes 1 or 2). This agreed with the sensitivity results; changes in AP C3-convertase formation affected the downstream dynamics of C5a formation. Thus, if we only considered the alternate pathway, C3 alone could be a reasonable target, especially given that C5a formation was surprisingly robust to C5 levels in the alternate pathway (Fig. 5A or B, lane 2). Yet, when both pathways were activated, C5a levels were robust to the initial C3 concentration (Fig. 5A or B, lane 4); C5a formation was catalyzed by CP C3 and C5 convertases. Thus, the only reliable intervention that consistently reduced both C3a and C5a formation for all cases was a dual-knockdown of C3 and C5. For example, a 90% decrease of both C3 and C5 reduced the formation of C5a by over an order of magnitude (Fig. 5B, lane 4), while C3a was reduced to a lesser extent (Fig. 5B, lane 3).

Discussion

In this study, we developed an ensemble of experimentally validated reduced order complement models. The modeling approach combined ordinary differential equations with logical rules to produce a complement model with a limited number of equations and parameters. The reduced order model, which described the lectin and alternative pathways, consisted of 18 differential equations with 28 parameters. Thus, the model was an order of magnitude smaller and included more pathways than comparable mathematical models in the literature. We estimated an ensemble of model parameters from *in vitro* time series measurements of the C3a and C5a complement proteins. Subsequently, we validated the model on unseen C3a and C5a measurements that were not used for model training. Despite its small size, the model was surprisingly predictive. After validation, we performed global sensitivity and robustness analysis to estimate which parameters and species controlled model performance. These analyses suggested complement was robust to any single therapeutic intervention. The only intervention that consistently reduced C5a formation for all cases was a dual-knockdown of both C3 and C5. Taken together, we developed a reduced order complement model that was computationally inexpensive, and could easily be incorporated into pre-existing or new pharmacokinetic models of immune system function. The model described experimental data, and predicted the need for multiple points of intervention to disrupt complement activation.

Despite its importance, there has been a paucity of validated mathematical models of complement pathway activation. To our knowledge, this study is one of the first complement models that combined multiple initiation pathways with experimental validation of important complement products like C5a. However, there have been several theoretical models of components of the cascade in the literature. Liu and co-workers modeled the formation of C3a through the classical pathway using 45 non-linear ODEs (19). In contrast, in this study we modeled lectin mediated C3a formation using only five ODEs.

11

Though we did not model all the initiation interactions in detail, especially the cross-talk between the lectin and classical pathways, we successfully captured C3a dynamics with respect to different concentrations of lectin initiators. The model also captured the dynamics of C3a and C5a formed from the alternate pathway using only seven ODEs. The reduced order model predictions of C5a were qualitatively similar to the theoretical complement model of Zewde et al which involved over 100 ODEs (16). However, we found that the quantity of C3a produced in the alternate pathway was nearly 1000 times the amount of C5a generated. While this was in agreement with the experimental data (20), it differed from the theoretical predictions made by Zewde et al. who showed C3a was 10^8 times greater than the C5a concentration (16). In our model, the time profile of both C3a and C5a generated changed with respect to the quantity of zymosan (the lectin pathway initiator). In particular, the C3a peak time was directly proportional to initiator, while the lag phase for generation was inversely proportional to the initiator concentration. Korotaevskiy et al. showed a similar trend using a theoretical model of complement, albeit for much shorter time scales (18). Thus, the reduced order complement model performed at least as well as existing larger mechanistic models, despite being significantly smaller.

Global analysis of the complement model suggested potentially important therapeutic targets. Complement malfunctions are implicated in a spectrum of diseases, however the development of complement specific therapeutics has been challenging (3, 21). Previously, we have shown that mathematical modeling and analysis can be useful tools to estimate therapeutically important mechanisms (22–25). In this study, we analyzed a validated ensemble of reduced order complement models to better understand the strengths and weaknesses of the cascade. In the presence of an initiator, C3a and C5a formation was sensitive to CP C3/C5 convertase assembly and activity, and to a lesser extent lectin initiation parameters. Formation of the CP convertases can be inhibited by targeting upstream protease complexes like MASP-1,2 from the lectin pathway (or C1r, C1s from

12

classical pathway). For example, Omeros, a protease inhibitor that targets the MASP-2 complex, has been shown to inhibit the formation of downstream convertases (26). Lampalizumab and Bikaciomab, which target factor B and factor D respectively, or naturally occurring proteins such as Cobra Venom Factor (CVF), an analogue of C3b, could also attenuate AP convertase formation (27–29). Removing supporting molecules could also destabilize the convertases. For example, Novelmed Therapeutics developed the antibody, NM9401 against propedin, a small protein that stabilizes alternate C3 convertase (30). Lastly, convertase catalytic activity could be attenuated using small molecule protease inhibitors. All of these approaches are consistent with the results of the sensitivity analysis. On the other hand, robustness analysis suggested C3a and C5a generation could be significantly attenuated by modulating the free levels of C3 and C5. The most commonly used anti-complement drug eculizumab, targets the C5 protein (21). A number of other drugs targeting C5 are also being developed. For example, LFG316 targets C5 in Age-Related Macular Degeneration (31), while Mubodina, an antibody that targets C5, is used to treat Atypical Hemolytic-Uremic Syndrome (aHUS) (32). Other agents such as the small molecule Coversin (33), the aptamer Zimura (34), as well as small peptides and RNAi could also be used to inhibit C5 (35). The cyclic peptide C3 inhibitor Compstatin and its derivatives [FINISH] (36). However, while the knockdown of C3 and C5 affects C3a and C5a levels downstream, the abundance and turnover rate of these proteins make them difficult to target (37, 38). For example, the eculizumab dosage needs to be adjusted while treating for Atypical Hemolytic-Uremic Syndrome (aHUS), a disease involving uncontrolled complement activation (39).

The performance of the complement model was impressive given its limited size. However, there are several questions that should be explored further. A logical progression for this work would be to expand the network to include the classical pathway and the formation of the membrane attack complex (MAC). However, it is unclear whether the addition

13

of the classical pathway will decrease the predictive quality of our existing model. Liu et al have shown cross-talk between the activation of the classical and lectin pathways that could influence model performance (19). One potential approach to address such difficulties would be to incorporate C reactive proteins (CRP) and L-ficolin (LF) into the model, both of which are involved with the initiation of classical and lectin pathways. Liu et al. showed that under inflammation conditions interactions between lectin and classical pathways was mediated through CRP and LF (19). Thus incorporating these two proteins would help us in modeling cross talk. Time course measurements of MAC abundance (and MAC formation dynamics) are also scarce, making the inclusion of MAC challenging. Next, we should address the under-prediction of C3a. We believe the C3a under-prediction can be attributed to how we modeled C4BP interactions. C4BP interactions were modeled as irreversible binding steps resulting in completely inactive complexes; however, the binding of C4BP with complement proteins is likely reversible and C4BP-bound convertases may have residual activity. We also did not capture the maximum concentration of C3a at low initiator levels. One possible reasons for this could the C2-by pass pathway, which was not included in the model. This pathway further accelerates C3a production without the involvement of a C3 convertase. Currently the C3a in the model is generated only through the activity of a C3 convertase. Incorporating this additional step within the reduced order modeling framework would be a future direction that we need to consider. We should test alternative model structures which include reversible C4BP binding, and partially active convertases. Alternatively, we could also perform sensitivity analysis on the C3a prediction residual to determine which parameters controlled the C3a prediction.

14

Materials and Methods

Formulation and solution of the complement model equations. We used ordinary differential equations (ODEs) to model the time evolution of complement proteins (x_i) in the reduced order model:

$$\frac{1}{\tau_i}\frac{dx_i}{dt} = \sum_{j=1}^{\mathcal{R}} \sigma_{ij} r_j\left(\mathbf{x}, \epsilon, \mathbf{k}\right) \qquad i = 1, 2, \ldots, \mathcal{M} \tag{1}$$

where $\mathcal{R}$ denotes the number of reactions and $\mathcal{M}$ denotes the number of protein species in the model. The quantity τ_i denotes a timescale parameter for species i which captures unmodeled effects; by default $\tau_i = 1$, for all species unless otherwise specified. The quantity $r_j\left(\mathbf{x}, \epsilon, \mathbf{k}\right)$ denotes the rate of reaction j. Typically, reaction j is a non-linear function of biochemical and enzyme species abundance, as well as unknown model parameters $\mathbf{k}$ ($\mathcal{K} \times 1$). The quantity σ_{ij} denotes the stoichiometric coefficient for species i in reaction j. If $\sigma_{ij} > 0$, species i is produced by reaction j. Conversely, if $\sigma_{ij} < 0$, species i is consumed by reaction j, while $\sigma_{ij} = 0$ indicates species i is not connected with reaction j. Species balances were subject to the initial conditions $\mathbf{x}\left(t_o\right) = \mathbf{x}_o$.

Rate processes were written as the product of a kinetic term ($\bar{r}_j$) and a control term (v_j) in the complement model. The kinetic term for the formation of C4a, C4b, C2a and C2b, lectin pathway activation, and C3 and C5 convertase activity was given by:

$$\bar{r}_j = k_j^{max} \epsilon_i \left(\frac{x_s^{\eta}}{K_{js}^{\eta} + x_s^{\eta}}\right) \tag{2}$$

where k_j^{max} denotes the maximum rate for reaction j, ϵ_i denotes the abundance of the enzyme catalyzing reaction j, η denotes a cooperativity parameter, and K_{js} denotes the saturation constant for species s in reaction j. We used mass action kinetics to model

protein-protein binding interactions within the network:

$$\bar{r}_j = k_j^{max} \prod_{s \in m_j^-} x_s^{-\sigma_{sj}} \tag{3}$$

where k_j^{max} denotes the maximum rate for reaction j, σ_{sj} denotes the stoichiometric coefficient for species s in reaction j, and $s \in m_j$ denotes the set of *reactants* for reaction j. We assumed all binding interactions were irreversible.

The control terms $0 \leq v_j \leq 1$ depended upon the combination of factors which influenced rate process j. For each rate, we used a rule-based approach to select from competing control factors. If rate j was influenced by $1, \ldots, m$ factors, we modeled this relationship as $v_j = \mathcal{I}_j (f_{1j} (\cdot), \ldots, f_{mj} (\cdot))$ where $0 \leq f_{ij} (\cdot) \leq 1$ denotes a regulatory transfer function quantifying the influence of factor i on rate j. The function $\mathcal{I}_j (\cdot)$ is an integration rule which maps the output of regulatory transfer functions into a control variable. Each regulatory transfer function took the form:

$$f_{ij} (\mathcal{Z}_i, k_{ij}, \eta_{ij}) = k_{ij}^{\eta_{ij}} \mathcal{Z}_i^{\eta_{ij}} / \left(1 + k_{ij}^{\eta_{ij}} \mathcal{Z}_i^{\eta_{ij}}\right) \tag{4}$$

where $\mathcal{Z}_i$ denotes the abundance of factor i, k_{ij} denotes a gain parameter, and η_{ij} denotes a cooperativity parameter. In this study, we used $\mathcal{I}_j \in \{min, max\}$ (40). If a process has no modifying factors, $v_j = 1$. The model equations were implemented in Julia and solved using the `CVODE` routine of the Sundials package (41, 42). The model code and parameter ensemble is freely available under an MIT software license and can be downloaded from http://www.varnerlab.org.

Estimating an ensemble of complement model parameters. We estimated a single initial parameter set using the Dynamic Optimization with Particle Swarms (DOPS) technique [REF]. DOPS is a novel hybrid meta-heuristic which combines a multi-swarm parti-

16

cle swarm method with the dynamically dimensioned search approach of Shoemaker and colleagues (43). DOPS minimized the squared residual between simulated and C3a and C5a measurements with and without zymosan as a single objective. The best fit set estimated by DOPS served as the starting point for multiobjective ensemble generation using Pareto Optimal Ensemble Technique in the Julia programming language (JuPOETs) (44). JuPOETs is a multiobjective approach which integrates simulated annealing with Pareto optimality to estimate model ensembles on or near the optimal tradeoff surface between competing training objectives. JuPOETs minimized training objectives of the form:

$$O_j(\mathbf{k}) = \sum_{i=1}^{\mathcal{T}_j} \left(\hat{\mathcal{M}}_{ij} - \hat{y}_{ij}(\mathbf{k}) \right)^2 + \left(\frac{\mathcal{M}'_{ij} - \max y_{ij}}{\mathcal{M}'_{ij}} \right)^2 \tag{5}$$

subject to the model equations, initial conditions and parameter bounds $\mathcal{L} \leq \mathbf{k} \leq \mathcal{U}$. The first term in the objective function measured the shape difference between the simulations and measurements. The symbol $\hat{\mathcal{M}}_{ij}$ denotes a scaled experimental observation (from training set j) while the symbol $\hat{y}_{ij}$ denotes the scaled simulation output (from training set j). The quantity i denotes the sampled time-index and $\mathcal{T}_j$ denotes the number of time points for experiment j. The scaled measurement is given by:

$$\hat{\mathcal{M}}_{ij} = \frac{\mathcal{M}_{ij} - \min_i \mathcal{M}_{ij}}{\max_i \mathcal{M}_{ij} - \min_i \mathcal{M}_{ij}} \tag{6}$$

Under this scaling, the lowest measured concentration become zero while the highest equaled one, where a similar scaling was defined for the simulation output. The second-term in the objective function quantified the absolute error in the estimated concentration scale, where the absolute measured concentration (denoted by $\mathcal{M}'_{ij}$) was compared with the largest simulated value. In this study, we minimized two training objectives, the total C3a and C5a residual w/o zymosan (O_1) and the total C3a and C5a residual for 1 mg/ml

17

zymosan (O_2). JuPOETs identified an ensemble of N $\simeq$ 2100 parameter sets which were used for model simulations and uncertainty quantification subsequently. JuPOETs is open source, available under an MIT software license. The JuPOETs source code is freely available from the JuPOETs GitHub repository at https://github.com/varnerlab/POETs.jl. The objective functions used in this study are available in the GitHub model repository available from http://varnerlab.org.

Sensitivity and robustness analysis of complement model performance. We conducted global sensitivity and robustness analysis to estimate which parameters and species controlled the performance of the reduced order model. We computed the total variance-based sensitivity index of each parameter relative to the training residual for the C3a/C5a alternate and C3a/C5a lectin objectives using the Sobol method (45). The sampling bounds for each parameter were established from the minimum and maximum value for that parameter in the parameter ensemble. We used the sampling method of Saltelli *et al.* to compute a family of $N(2d+2)$ parameter sets which obeyed our parameter ranges, where N was the number of trials per parameters, and d was the number of parameters in the model (46). In our case, N = 400 and d = 28, so the total sensitivity indices were computed using 23,200 model evaluations. The variance-based sensitivity analysis was conducted using the SALib module encoded in the Python programming language (47).

Robustness coefficients quantify the response of a marker to a structural or operational perturbation to the network architecture. Robustness coefficients were calculated as shown previously (48). Log-transformed robustness coefficients denoted by $\hat{\alpha}(i, j, t_o, t_f)$ are defined as:

$$\hat{\alpha}(i, j, t_o, t_f) = \log_{10}\left[\left(\int_{t_o}^{t_f} x_i(t)\, dt\right)^{-1}\left(\int_{t_o}^{t_f} x_i^{(j)}(t)\, dt\right)\right] \tag{7}$$

Here t_o and t_f denote the initial and final simulation time, while i and j denote the indices

for the marker and the perturbation, respectively. A value of $\hat{\alpha}\left(i, j, t_o, t_f\right) > 0$, indicates increased marker abundance, while $\hat{\alpha}\left(i, j, t_o, t_f\right) < 0$ indicates decreased marker abundance following perturbation j. If $\hat{\alpha}\left(i, j, t_o, t_f\right) \sim 0$, perturbation j did not influence the abundance of marker i. In this study, we perturbed the initial condition of C3 or C5 or a combination of C3 and C5 by 50% or 90% and measured the area under the curve (AUC) of C3a or C5a with and without lectin initiator. Log-transformed robustness coefficients were calculated for every member of the ensemble, where the mean $\pm$ 1×standard-deviation are reported.

Competing interests

The authors declare that they have no competing interests.

Author's contributions

J.V directed the study. A.S developed the reduced order complement model and the parameter ensemble. A.S, W.D and M.M analyzed the model ensemble, and generated figures for the manuscript. The manuscript was prepared and edited for publication by A.S, W.D, M.M and J.V.

Acknowledgements

Funding

References

1. Nuttall G (1888) Experimente über die bacterienfeindlichen Einflüsse des thierischen Körpers. Z Hyg Infektionskr 4: 353-394.

2. Ricklin D, Hajishengallis G, Yang K, Lambris JD (2010) Complement: a key system for immune surveillance and homeostasis. NAT IMMUNOL 11: 785–797.

3. Ricklin D, Lambris JD (2007) Complement-targeted therapeutics. NAT BIOTECHNOL 25: 1265-1275.

4. Rittirsch D, Flierl MA, Ward PA (2008) Harmful molecular mechanisms in sepsis. NAT REV IMMUNOL 8: 776–787.

5. Sarma JV, Ward PA (2011) The complement system. Cell Tissue Res 343: 227–235.

6. Ricklin D, Lambris JD (2013) Complement in immune and inflammatory disorders: pathophysiological mechanisms. J Immunol 190: 3831–3838.

7. Walport MJ (2001) Complement. first of two parts. N Engl J Med 344: 1058-66.

8. Walport MJ (2001) Complement. second of two parts. N Engl J Med 344: 1140-4.

9. Pangburn MK, Müller-Eberhard HJ (1984) The alternative pathway of complement. Semin Immunopathol .

10. Walker D, Yasuhara O, Patston P, McGeer E, McGeer P (1995) Complement c1 inhibitor is produced by brain tissue and is cleaved in alzheimer disease. Brain Res 675: 75–82.

11. Blom AM, Kask L, Dahlbäck B (2001) Structural requirements for the complement regulatory activities of c4bp. J Biol Chem 276: 27136–27144.

12. Riley-Vargas RC, Gill DB, Kemper C, Liszewski MK, Atkinson JP (2004) Cd46: expanding beyond complement regulation. Trends Immunol 25: 496–503.

13. Lukacik P, Roversi P, White J, Esser D, Smith G, et al. (2004) Complement regulation at the molecular level: the structure of decay-accelerating factor. Proc Natl Acad Sci USA 101: 1279–1284.

472 14. Liszewski MK, Farries TC, Lublin DM, Rooney IA, Atkinson JP (1995) Control of the
473   complement system. Adv Immunol 61: 201–283.

474 15. Chauhan A, Moore T (2006) Presence of plasma complement regulatory proteins
475   clusterin (apo j) and vitronectin (s40) on circulating immune complexes (cic). Clin
476   Exp Immunol 145: 398–406.

477 16. Zewde N, Gorham Jr RD, Dorado A, Morikis D (2016) Quantitative modeling of the
478   alternative pathway of the complement system. PloS one 11: e0152337.

479 17. Hirayama H, Yoshii K, Ojima H, Kawai N, Gotoh S, et al. (1996) Linear systems analy-
480   sis of activating processes of complement system as a defense mechanism. Biosys-
481   tems 39: 173–185.

482 18. Korotaevskiy AA, Hanin LG, Khanin MA (2009) Non-linear dynamics of the comple-
483   ment system activation. Math Biosci 222: 127–143.

484 19. Liu B, Zhang J, Tan PY, Hsu D, Blom AM, et al. (2011) A computational and experi-
485   mental study of the regulatory mechanisms of the complement system. PLoS Comput
486   Biol 7: e1001059.

487 20. Morad HO, Belete SC, Read T, Shaw AM (2015) Time-course analysis of c3a and
488   c5a quantifies the coupling between the upper and terminal complement pathways in
489   vitro. J Immunol Methods 427: 13–18.

490 21. Morgan BP, Harris CL (2015) Complement, a target for therapy in inflammatory and
491   degenerative diseases. NAT REV DRUG DISCOV 14: 857-877.

492 22. Luan D, Zai M, Varner JD (2007) Computationally derived points of fragility of a human
493   cascade are consistent with current therapeutic strategies. PLoS Comput Biol 3:
494   e142.

495 23. Nayak S, Salim S, Luan D, Zai M, Varner JD (2008) A test of highly optimized tol-
496   erance reveals fragile cell-cycle mechanisms are molecular targets in clinical cancer
497   trials. PLoS One 3: e2016.

24. Tasseff R, Nayak S, Salim S, Kaushik P, Rizvi N, et al. (2010) Analysis of the molecular networks in androgen dependent and independent prostate cancer revealed fragile and robust subsystems. PLoS One 5: e8864.

25. Rice NT, Szlam F, Varner JD, Bernstein PS, Szlam AD, et al. (2016) Differential contributions of intrinsic and extrinsic pathways to thrombin generation in adult, maternal and cord plasma samples. PLoS One 11: e0154127.

26. Schwaeble HW, Stover CM, Tedford CE, Parent JB, Fujita T (2011). Methods for treating conditions associated with masp-2 dependent complement activation. US Patent 7,919,094.

27. Vogel CW, Fritzinger DC, Hew BE, Thorne M, Bammert H (2004) Recombinant cobra venom factor. Molecular immunology : 191–199.

28. Katschke KJ, Wu P, Ganesan R, Kelley RF, Mathieu MA, et al. (2012) Inhibiting alternative pathway complement activation by targeting the factor d exosite. Journal of Biological Chemistry : 12886–12892.

29. Hu X, Holers VM, Thurman JM, Schoeb TR, Ramos TN, et al. (2013) Therapeutic inhibition of the alternative complement pathway attenuates chronic eae. Mol Immunol : 302–308.

30. Bansal R (2014). Humanized and chimeric anti-properdin antibodies. US Patent 8,664,362.

31. Roguska M, Splawski I, Diefenbach-Streiber B, Dolan E, Etemad-Gilbertson B, et al. (2014) Generation and characterization of lfg316, a fully-human anti-c5 antibody for the treatment of age-related macular degeneration. Investigative Ophthalmology & Visual Science : 3433–3433.

32. Melis JP, Strumane K, Ruuls SR, Beurskens FJ, Schuurman J, et al. (2015) Complement in therapy and disease: Regulating the complement system with antibody-based therapeutics. Molecular immunology : 117–130.

524 33. Weston-Davies WH, Nunn MA, Pinto FO, Mackie IJ, Richards SJ, et al. (2014) Clini-
525 cal and immunological characterisation of coversin, a novel small protein inhibitor of
526 complement c5 with potential as a therapeutic agent in pnh and other complement
527 mediated disorders. Blood : 4280–4280.

528 34. Epstein D, Kurz JC (2007). Complement binding aptamers and anti-c5 agents useful
529 in the treatment of ocular disorders. US Patent App. 12/224,708.

530 35. Borodovsky A, Yucius K, Sprague A, Banda NK, Holers VM, et al. (2014) Aln-cc5, an
531 investigational rnai therapeutic targeting c5 for complement inhibition. Complement
532 20: 40.

533 36. Mastellos DC, Yancopoulou D, Kokkinos P, Huber-Lang M, Hajishengallis G, et al.
534 (2015) Compstatin: a c3-targeted complement inhibitor reaching its prime for bedside
535 intervention. Eur J Clin Invest 45: 423-40.

536 37. Sissons J, Liebowitch J, Amos N, Peters D (1977) Metabolism of the fifth component
537 of complement, and its relation to metabolism of the third component, in patients with
538 complement activation. J Clin Invest 59: 704.

539 38. Swaak A, Hannema A, Vogelaar C, Boom F, van Es L, et al. (1982) Determination of
540 the half-life of c3 in patients and its relation to the presence of c3-breakdown products
541 and/or circulating immune complexes. Rheumatol Int : 161–166.

542 39. Noris M, Galbusera M, Gastoldi S, Macor P, Banterla F, et al. (2014) Dynamics of
543 complement activation in ahus and how to monitor eculizumab therapy. Blood : 1715–
544 1726.

545 40. Sagar A, Varner JD (2015) Dynamic modeling of the human coagulation cascade
546 using reduced order effective kinetic models. Processes 3: 178.

547 41. Bezanson J, Edelman A, Karpinski S, Shah VB (2015) Julia: A fresh approach to
548 numerical computing .

549 42. Hindmarsh AC, Brown PN, Grant KE, Lee SL, Serban R, et al. (2005) Sundials: Suite

24

550 of nonlinear and differential/algebraic equation solvers. ACM Trans Math Softw 31:

551 363–396.

43. Tolson BA, Shoemaker CA (2007) Dynamically dimensioned search algorithm for computationally efficient watershed model calibration. Water Resources Research 43: W01413.

44. Bassen D, Vilkhovoy M, Minot M, Butcher JT, Varner JD (2016) Jupoets: A constrained multiobjective optimization approach to estimate biochemical model ensembles in the julia programming language. bioRxiv .

45. Sobol I (2001) Global sensitivity indices for nonlinear mathematical models and their monte carlo estimates. MATH COMPUT SIMULAT 55: 271 - 280.

46. Saltelli A, Annoni P, Azzini I, Campolongo F, Ratto M, et al. (2010) Variance based sensitivity analysis of model output. design and estimator for the total sensitivity index. Comput Phys Commun 181: 259–270.

47. Herman J. Salib: Sensitivity analysis library in python (numpy). contains sobol, morris, fractional factorial and fast methods. available online: https://github.com/jdherman/salib.

48. Tasseff R, Nayak S, Song SO, Yen A, Varner JD (2011) Modeling and analysis of retinoic acid induced differentiation of uncommitted precursor cells. Integr Biol (Camb) 3: 578-91.
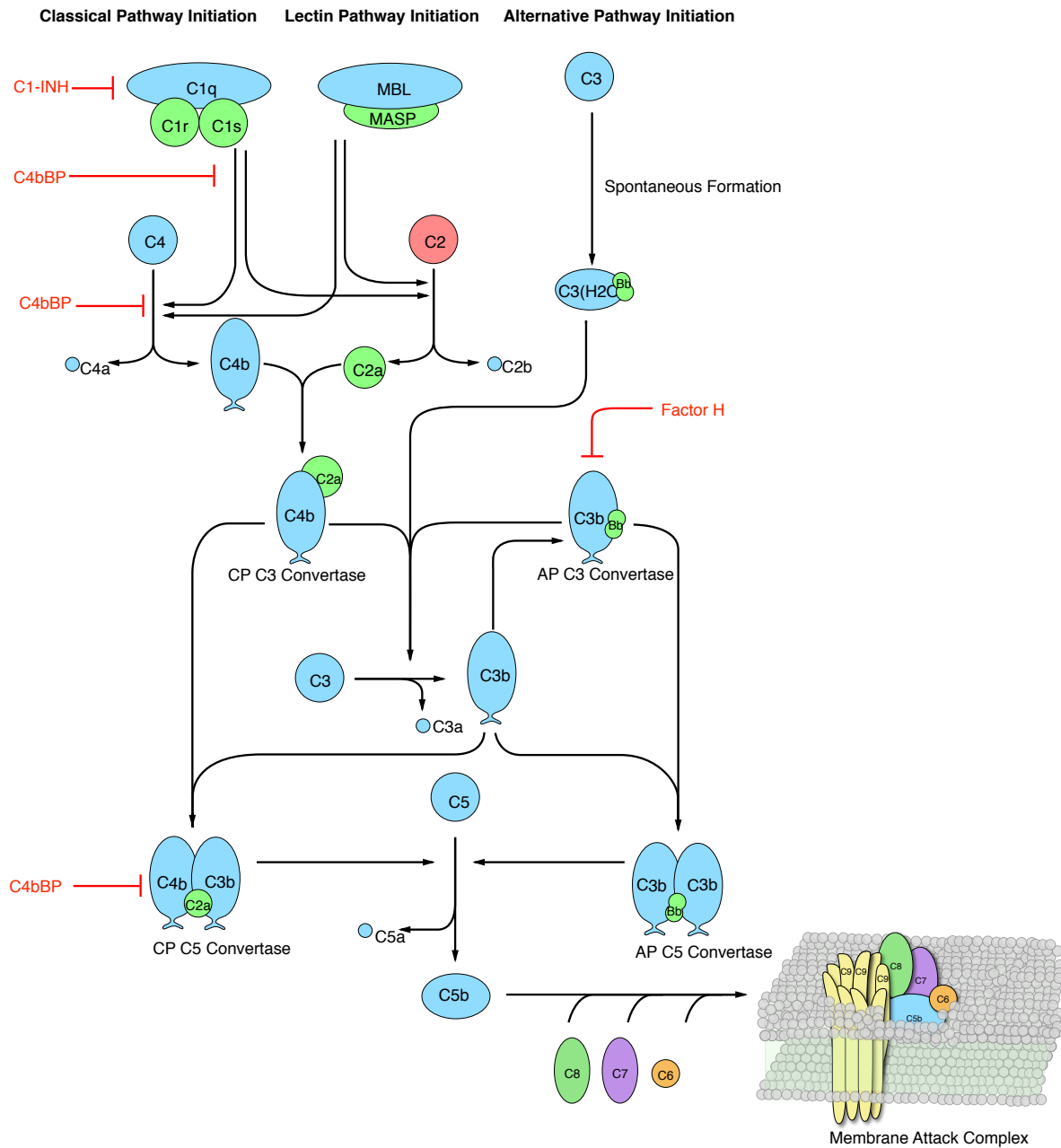
Fig. 1: Simplified schematic of the human complement system. The complement cascade is activated through three pathways: the classical, the lectin, and the alternate pathways. Complement initiation results in the formation of classical or alternative C3 convertases, which amplify the initial complement response and signal to the adaptive immune system by cleaving C3 into C3a and C3b. C3 convertases further react to form C5 convertases which catalyze the cleavage of the C5 complement protein to C5a and C5b. C5b is critical to the formation of the membrane attack complex (MAC), while C5a recruits an adaptive immune response.
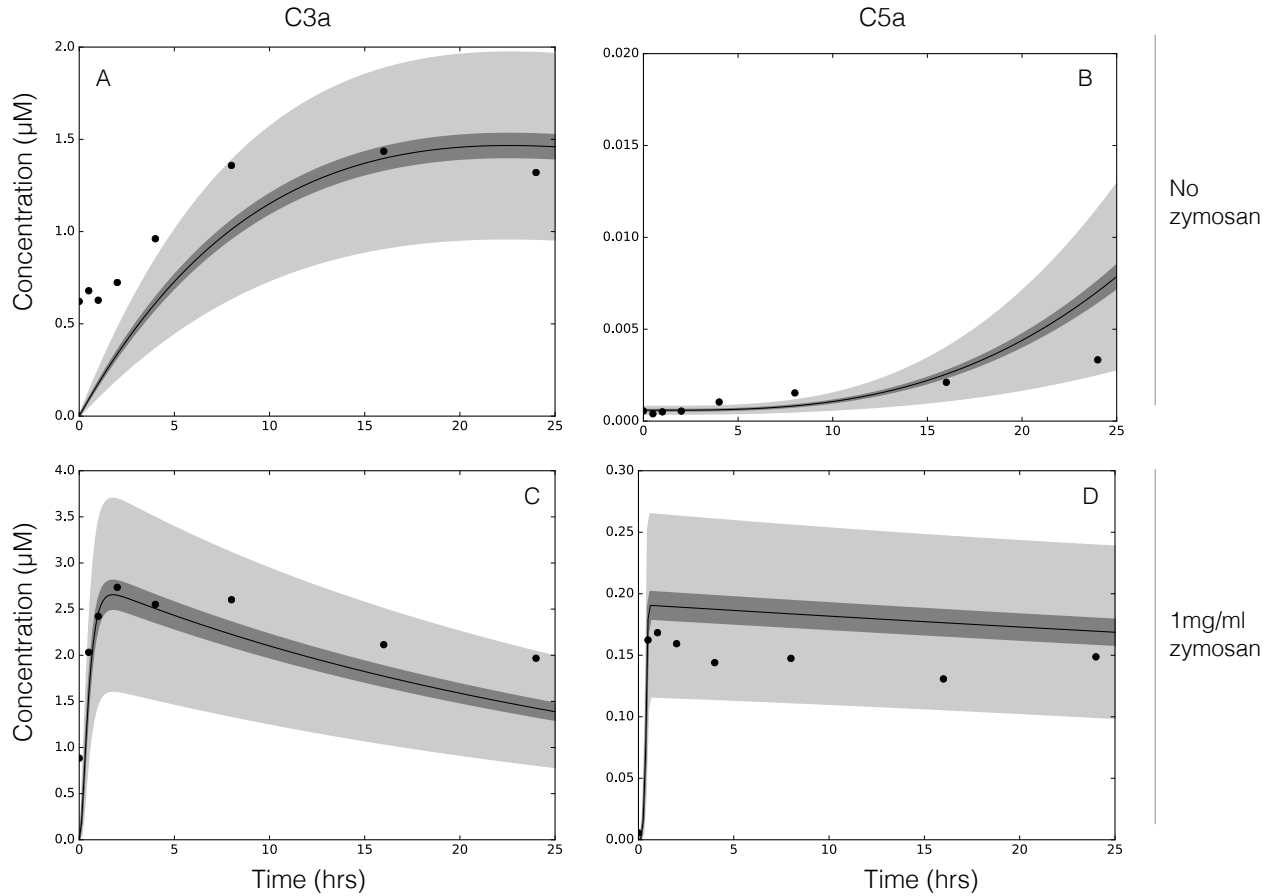
Fig. 2: Reduced order complement model training. Model parameters were estimated using Dynamic Optimization with Particle Swarms (DOPS) from C3a and C5a measurements with and without zymosan (20). The model was trained using C3a and C5a data generated from the alternative pathway (**A**–**B**) and lectin pathway initiated with 1g zymosan (**C**–**D**). The solid red line shows the simulation with the best-fit parameter set, the solid black lines show the simulated mean value of C3a or C5a for the ensemble (N = 50). The dark shaded region denotes the 99% confidence interval of the simulated mean concentrations, while the light shaded region denotes the 99% confidence interval of the best-fit simulation for C3a and C5a. All initial conditions were assumed to be at their physiological serum levels unless otherwise noted.
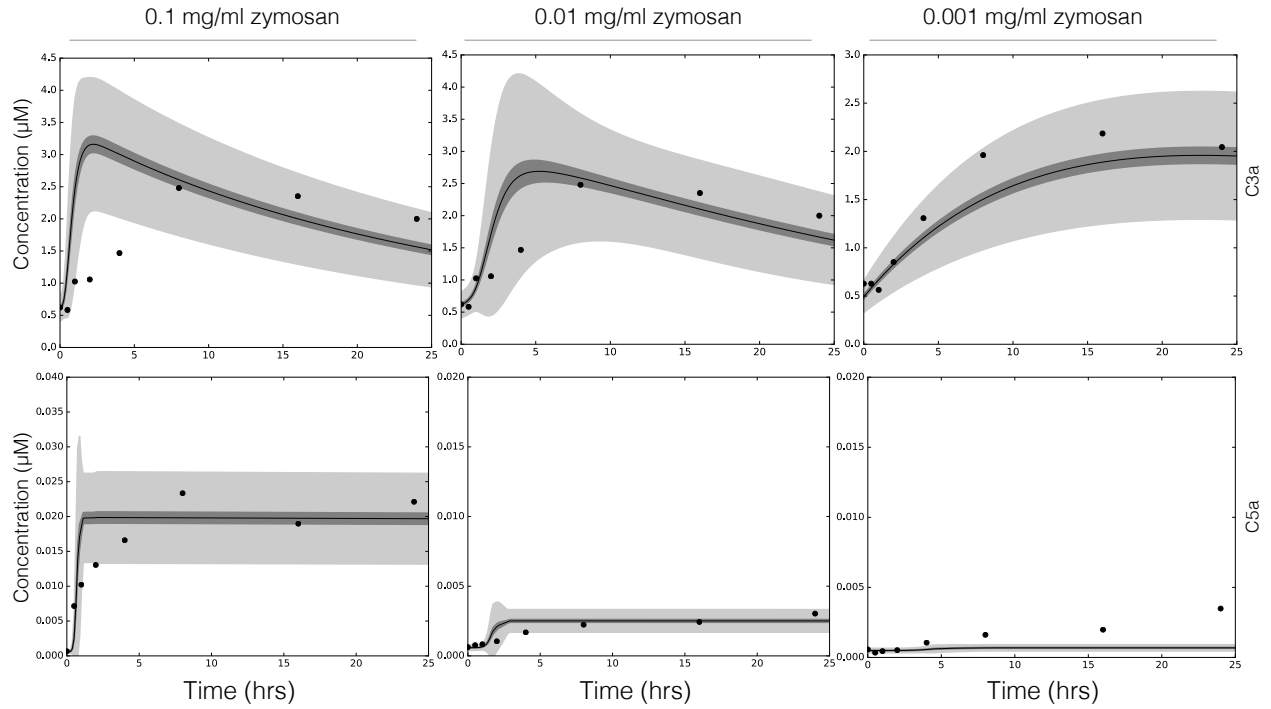
Fig. 3: Reduced order complement model predictions. The reduced order coagulation model parameter estimates were tested against data not used during model training (20). Simulations of C3a and C5a generated in the lectin pathway using 0.1g, 0.01g, and 0.001g zymosan were compared with the corresponding experimental measurement. The solid red line shows the simulation with the best-fit parameter set, the solid black lines show the simulated mean value of C3a or C5a for the ensemble (N = 50). The dark shaded region denotes the 99% confidence interval of the simulated mean concentrations, while the light shaded region denotes the 99% confidence interval of the best-fit simulation for C3a and C5a. All initial conditions were assumed to be at their physiological serum levels unless otherwise noted.
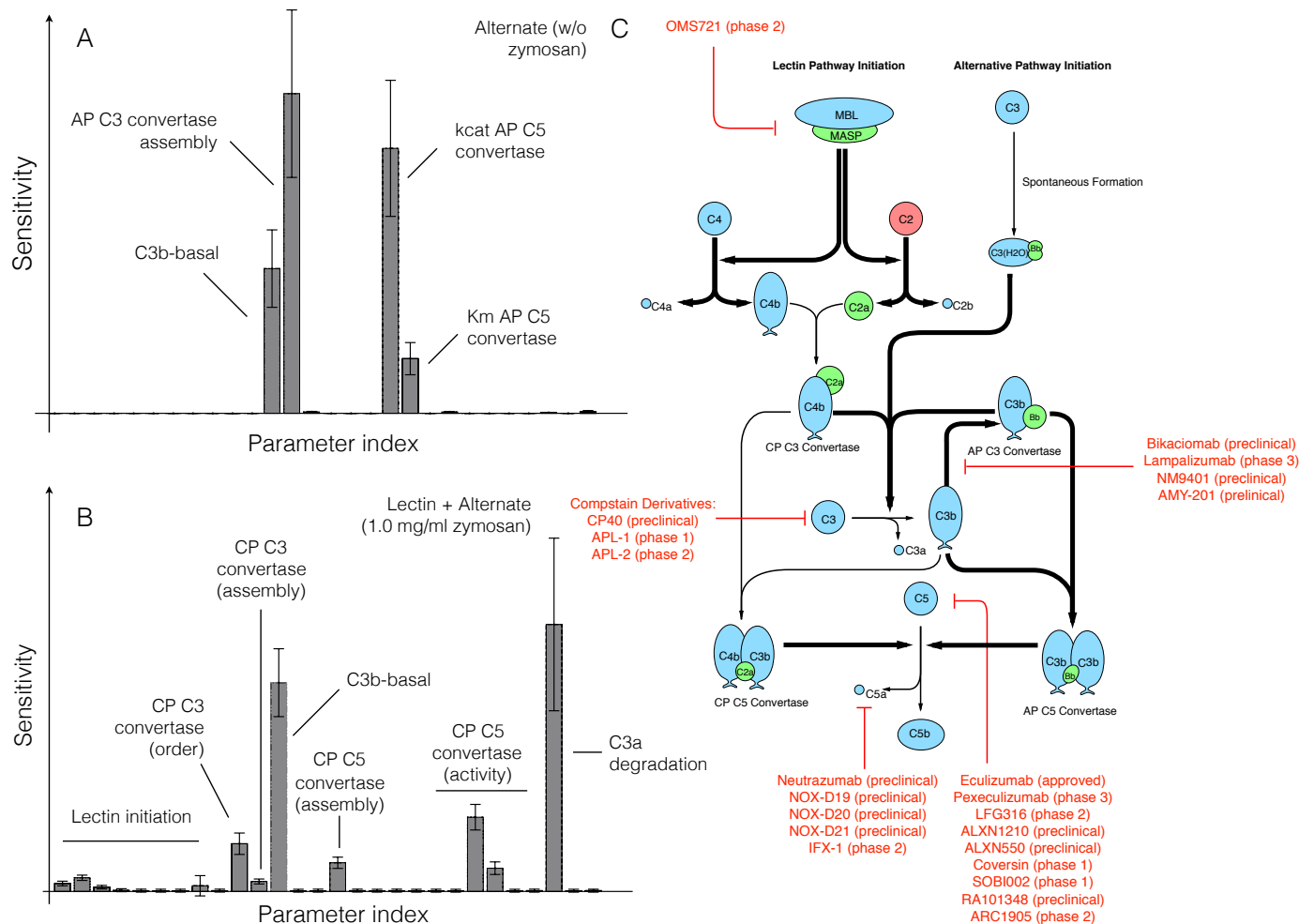
Fig. 4: Global sensitivity analysis of the reduced order complement model. Sensitivity analysis was conducted on the two objectives used for model training. **A**: Sensitivity of the C3a and C5a residual w/o zymosan, **B**: Sensitivity of the C3a and C5a residual with 1mg/ml zymosan. The bars denote the mean total sensitivity index for each parameter, while the error bars denote the 95% confidence interval. **C**: Pathways controlled by the sensitivity parameters. Bold black lines indicate the pathway involves one or more sensitive parameters, while the red lines show current therapeutics targets. Current complement therapeutics were taken from the review of Morgan and Harris (21).
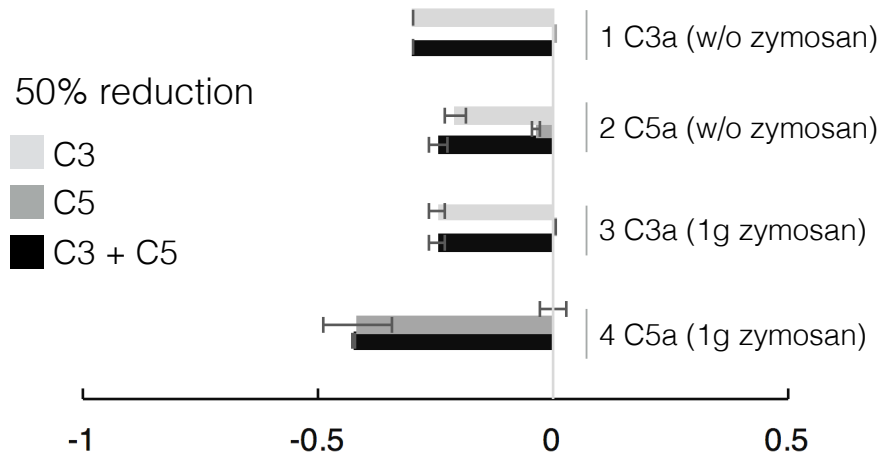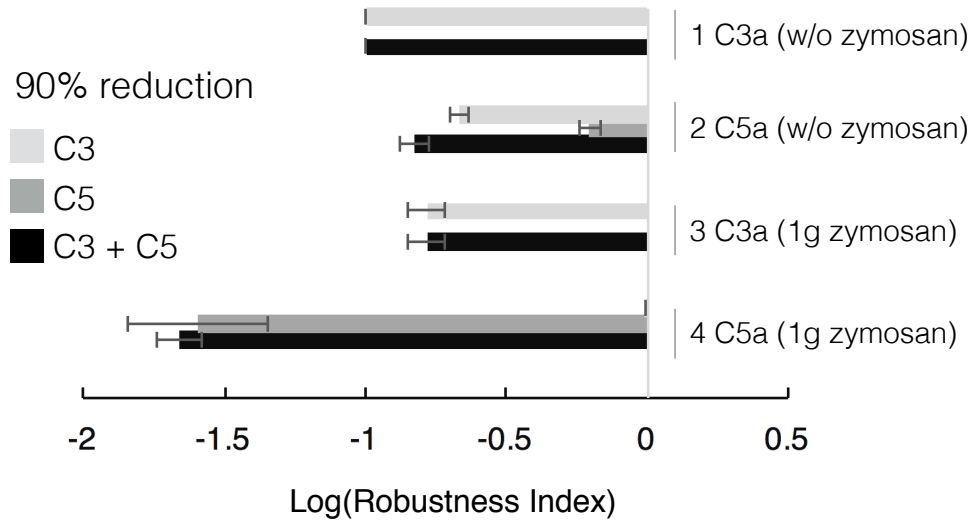
Fig. 5: Robustness analysis of the complement model with respect to C3 and C5 initial conditions. Robustness analysis was conducted on the four cases used for model training: C3a alternate (w/o zymosan), C5a alternate (w/o zymosan), C3a lectin (1g zymosan), and C5a lectin (1g zymosan), by reducing the initial concentration of C3 and/or C5 by 50% or 90 %. **A**: Robustness results for a 50% decrease in the C3, C5, or C3 and C5 initial condition. **B**: Robustness results for a 90% decrease in the C3, C5, or C3 and C5 initial condition. The bars denote the log-transformated robustness index while error bars denote one standard deviation. At zero, the perturbed initial concentration has no impact on the measured output. A log-transformed robustness index less than zero indicates a negative relation between the perturbed initial concentration and the measured output.